Spatiotemporal amplitude-and-phase reconstruction by Fourier-transform of interference spectra of high-complex-beams

Benjamín Alonso,[1,*] Íñigo J. Sola,[1] Óscar Varela,[1] Juan Hernández-Toro,[1] Cruz Méndez,[2] Julio San Román,[1] Amelle Zaïr,[1] and Luis Roso[2]

[1]*Universidad de Salamanca, Área de Óptica, Departamento de Física Aplicada, E-37008 Salamanca, Spain*
[2]*Centro de Láseres Pulsados Ultracortos Ultraintensos (CLPU), E-37008 Salamanca, Spain*
[*]*Corresponding author: b.alonso@usal.es*

Received November 23, 2009; revised February 11, 2010; accepted March 3, 2010;
posted March 4, 2010 (Doc. ID 120323); published April 20, 2010

We propose what we believe to be a novel method to reconstruct the spatiotemporal amplitude and phase of the electric field of ultrashort laser pulses using spatially resolved spectral interferometry. This method is based on a fiber-optic coupler interferometer that has certain advantages in comparison with standard interferometer systems, such as being alignment-free and selection of the reference beam at a single point. Our technique, which we refer to as the SpatioTemporal Amplitude-and-phase Reconstruction by Fourier-transform of Interference Spectra of High-complex-beams, offers compactness and simplicity. We report its application to the experimental characterization of chirped pulses and to spatiotemporal reconstructions of a convergent beam as well as plane-plane and spherical-plane waves interferences, which we check with our simulations. © 2010 Optical Society of America

OCIS codes: 320.7100, 120.3180, 260.3160, 140.3295.

1. INTRODUCTION

Laser pulse characterization is a fundamental issue for the extensive community of laser users. Knowledge of the structure of laser beams before they are used in certain experiments or applications and the study of the pulse after it has undergone a given process, are essential. However, the complexity of the electric field requires certain specific approaches when addressing it. The electric field of the light is in general a vector that depends on time and three spatial variables (two transverse directions and the longitudinal direction of propagation). We shall neglect the vectorial character of the electric field because here we are dealing with linearly polarized pulses.

The temporal variation and the spatial profile of ultrashort laser pulses are often characterized separately. Thus, the temporal characterization of pulses has a fairly long history. Pulse autocorrelation can afford an idea of the laser pulse duration and form [1]. Several robust and reliable techniques are now well established for the amplitude-and-phase retrieval, such as the frequency resolved optical gating (FROG) [2], spectral phase interferometry for direct electric-field reconstruction (SPIDER) [3], spectral interferometry (SI) [4,5], and its combination with the FROG, known as the temporal analysis by dispersing a pair of light electric fields [6]. Additionally, the spatial profile can be measured with a standard detector [a charge-coupled device (CCD)], but the spatial phase (i.e., the wave-front) can also be measured with different techniques, e.g., Hartmann–Shack [7].

One approach to the study of spatiotemporal evolution consists of measuring the temporal pulse profile at different spatial positions with SPIDER [8,9], and the grating-eliminated no-nonsense observation of ultrafast incident laser light electric fields [GRENOUILLE (single-shot FROG)] can also be used to measure the pulse-front tilt [10]. Nevertheless, in spite of being very useful these techniques cannot measure the full spatiotemporal information and preserve the coupling. The aim of our work is to develop a simple and robust system capable of reconstructing the spatiotemporal amplitude and phase of laser pulses at a fixed propagation distance. Our underlying motivation is the broad variety of application fields of spatiotemporal characterization, such as the study of optical aberrations [11,12] or nonlinear propagation [13–15].

Initial schemes for this purpose were based on the spatially resolved SI and did not characterize the reference beam, thus only measuring phase differences and being unable to perform complete spatiotemporal reconstructions [11,15]. The spatially resolved SI consists of measuring the spectral interferences of a test and a reference beam across the spatial profile. If the spatio-spectral phase of the reference beam is known, the spatiotemporal coupled amplitude and the phase of the test pulse can be retrieved. In the scheme of Diddams *et al.* [16], a Mach–Zehnder interferometer was used. Those authors filtered the reference beam spatially and measured it in a single position, assuming a constant spectral phase. In a previous work, we implemented the same scheme and found

that the spatial cleaning of the reference beam is not easy and does not ensure a perfectly homogeneous reference, especially when filtering complex pulses [17].

The amplitude-and-phase reconstruction of spatiotemporal coupling was studied by Rivet *et al.* [18], using a combination of Hartmann–Shack and FROG or SPIDER. This scheme, known as the Shackled-FROG, has recently been demonstrated by Rubino *et al.* [19]. A robust technique used by Dorrer *et al.* consisted of two-dimensional (spatial and spectral) shearing interferometry [20]. More recently, a holographic method reported by Gabolde and Trebino, spatially and temporally resolved intensity and phase evaluation device: full information from a single hologram (STRIPED FISH) [21] has demonstrated the ability to measure three-dimensional (x,y,t) electric fields in single-shot. To study nonlinear propagation, Trull *et al.* developed a technique that measures the spatially resolved temporal cross-correlation [13], measuring the sum frequency with a short probe. This technique provides an image of the spatiotemporal intensity (but not the phase), which is valuable information that has been used for measurements of X-waves [14].

Another recent technique is based on the spatially encoded arrangement temporal analysis by dispersing a pair of light electric fields (SEA TADPOLE) [22] scanning the test beam as proposed by Bowlan *et al.* [12]. The SEA TADPOLE technique measures the spectrally resolved spatial interferences of two non-delayed crossed beams. This idea had already been implemented by Meshulach *et al.* [23] in a primitive scheme involving crossing the beams directly and has been adapted by Bowlan *et al.* [12] by guiding a spatial selection of each beam (test and reference) with equal-length single-mode optical fibers. The temporal profile of the test beam is recovered from the spatio-spectral trace, hence with the advantage of using the full spectrometer resolution. The extension to spatiotemporal characterization merely consists of scanning the test beam profile with the fiber.

In this contribution, we report a novel scheme for the spatially resolved SI based on a fiber-optic coupler interferometer that has certain advantages in comparison with standard interferometers. We refer to it as the spatiotemporal amplitude-and-phase reconstruction by Fourier-transform of interference spectra of high-complex-beams (STARFISH).

Our system bears some similarities to the SEA TADPOLE since the test and reference beams are collected with optical fiber inputs: both systems are free of alignment and use a single reference pulse. The main differences are that our system is based on SI instead of spatial interferences [spatially encoded arrangement (SEA)] and that the STARFISH only uses a fiber coupler and a standard spectrometer. This makes our system very simple and robust in experimental terms, and its implementation or upgrading in a laboratory in a plug-and-play scheme is easier (simply plugging the coupler to the spectrometer). Moreover, the STARFISH measures a single spectrum for each spatial point (instead of a spatio-spectral trace), thereby reducing the data processing, which would be more interesting—for example—when measuring many spatial points at different propagation distances. Despite this, the use of the standard SI instead of spatial arrangements (SEA) involves a loss of spectrometer resolution, thus limiting the pulse length capable of being measured with the STARFISH in comparison with the SEA TADPOLE [22] and SEA SPIDER [24], although we shall show that this is not a problem.

2. SPATIALLY RESOLVED SPECTRAL INTERFEROMETRY

A. Spectral Interferometry

In SI, two beams (test and reference) are delayed with respect to each other by a time τ and propagate collinearly. The resulting spectrum of both beams is the sum of the spectra plus an interference term containing the information of the phase difference between the beams, as seen in Eq. (1). The interference fringes have a period given by the inverse of the delay. For the sign, we chose the criterion that the reference always goes before the test and the delay is positive. The resulting spectrum is

$$S(\omega) = S_{\text{test}}(\omega) + S_{\text{ref}}(\omega) + 2\sqrt{S_{\text{test}}(\omega)S_{\text{ref}}(\omega)}\cos[\phi_{\text{test}}(\omega) - \phi_{\text{ref}}(\omega) - \omega\tau]. \tag{1}$$

The fringe-inversion technique, the so-called Fourier-transform spectral interferometry (FTSI) [25], can be applied to retrieve the phase information. The inverse Fourier-transform affords three peaks in the temporal domain: one centered at $t=0$, coming from the continuum spectra (test and reference spectra), and two side-peaks centered at $t=\pm\tau$, corresponding to the interference term. The continuum contribution ($t=0$) can be depleted by subtracting the test and reference spectra from the interference spectrum. One side-peak is filtered and returned to the spectral domain by direct Fourier-transform, from where the phase difference between the test and reference beams is extracted. The time delay τ must be high enough to prevent central- and side-peak overlap, but small enough to allow the fringes to be resolved by the spectrometer. The reference spectrum must at least comprise the whole test spectrum and the spectral amplitudes should be comparable to have well contrasted fringes. If the reference phase is known, the test spectral phase can be calculated and, together with the test spectrum, the beam can be fully characterized in the temporal domain simply by applying a Fourier-transform. The delay is calculated from the side-peak position at a certain point and the term $\omega\tau$ is added to the retrieved phase.

The extension of the SI to spatiotemporal characterization in standard interferometer schemes is achieved by a spatial reference that is delayed with regard to the test beam as shown in Fig. 1. The reference beam must be spatially homogeneous (a flat wave-front and a spectral phase independent of the transverse position) because in general it can only be characterized at a single point. In this scheme, the test beam is referenced at each spatial position by a known pulse (thanks to the homogeneous spatiotemporal reference beam) and hence the connection between different spatial points in the test profile can be obtained. Accordingly, the experimental measurements consist of measuring the spectral interferences as a function of the scanned transverse position of the beam pro-

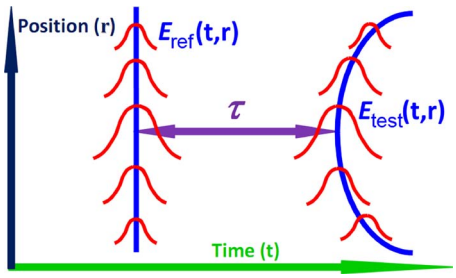

Fig. 1. (Color online) Scheme of spatiotemporal reference for spatially resolved SI, consisting of using a homogeneous flat reference beam delayed with respect to the test beam and scanning the position (transverse), and measuring their respective spectral interferences. Thus, each spatial position is referenced by a known pulse.

file, that is, spatio-spectral traces depending on the position and the wavelength. In Eq. (1), this involves the spectral amplitude and phase as functions of the wavelength and the transverse position. The spatially resolved spectrum (spectral trace) of the test arm is also measured, which—together with the spectral phase retrieved by the FTSI—allows the test beam to be characterized.

B. Experimental Setup for STARFISH: The Fiber-Optic Coupler

To avoid the complications of standard interferometer-based systems (homogeneous reference, precise alignment, etc.), here we propose an interferometer based on a fiber-optic coupler for the SI (STARFISH). The fiber coupler must be single-mode to avoid different mode dispersions. The fiber coupler was designed to work within a broadband spectral region ranging from 680 to 900 nm, allowing the characterization of ultrashort pulses. The configuration of the fiber coupler comprises two input ports and a common output port. The reference and test beams enter through each input port, are coupled in the transition, and exit the fiber, delayed, through the same port. In the experimental scheme (Fig. 2), the unknown beam is split, with each replica being sent to each fiber arm. The test arm fiber input has a motorized stage for the spatial scan (transverse), whereas the position of the fiber for the reference arm controls the delay between the pulses (longitudinal). The reference arm selects a suitable spatial position containing all spectral components that the test beam has at any position. This reference is characterized temporally with the FROG or SPIDER technique. Since the reference beam is not spatially scanned

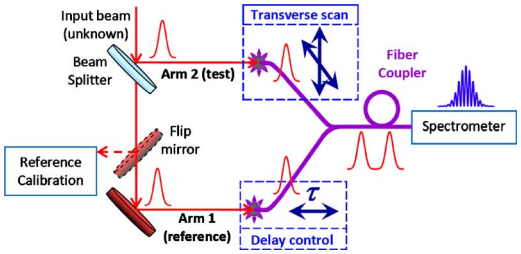

Fig. 2. (Color online) Setup based on the fiber-optic coupler interferometer for spatially resolved SI. The longitudinal position of one fiber arm controls the relative delay between reference and test beams. The test beam is scanned transversely (spatial) with its corresponding input fiber arm.

with the fiber input, only one point of the reference profile is selected with the fiber, and this allows a constant reference to be used instead of a possibly inhomogeneous reference profile. Thus, here we did not implement any spatial filtering because it was not necessary. Following the scheme shown in Fig. 1, our proposal consisted of referencing all the positions of the test beam by a single spatial point of the reference beam.

The arms of the fiber coupler should be of equal lengths (this does not exactly occur in reality) in order to avoid introducing different dispersions on the beams. Nevertheless, we consistently calibrated the global phase difference of the fiber coupler (due to slight differences in the lengths of the arms of the fiber coupler) and the beam splitter. This calibration was accomplished by taking a SI interferometry measurement using the same input beam in both arms. It was then taken into account in the reconstruction algorithm to retrieve the correct spectral phase.

The main advantages of this system are its simplicity, compactness, the fact that alignment is not necessary, the ease with which it can be upgraded simply by connecting the coupler to a different spectrometer, and the fact that a constant reference is used (we selected the broadest spectrum region). This means that we do not need a spatial filter for the reference, and approximations concerning reference homogeneity are required. In comparison with standard interferometers, we do not need a spatially homogeneous reference beam with at least the same spatial section and spectrum as the test beam. Moreover, the spatial resolution is given by the mode-field diameter of the single-mode fiber: in our case 4 μm.

3. EXPERIMENTAL MEASUREMENTS

A. Introduction

The experiments were carried out using two different terawatt-class Ti:Sapphire chirped pulse amplification (CPA) laser systems (both at a 10 Hz repetition rate). The first system (Spectra Physics, Inc.) delivers laser pulses of 120 fs (Fourier limit) with its spectrum centered at 795 nm. The second system (Amplitude Technologies) provides 35 fs pulses centered at 805 nm. We worked with two different lasers to test the STARFISH with pulses of different durations and bandwidths. For the temporal characterization of the reference beam we used the GRENOUILLE (single-shot FROG, Swamp Optics) and SPIDER (APE GmbH) devices, whereas for the spectra we used a commercial spectrometer (AVANTES, Inc.). Depending on the duration of the pulses, we characterized them with the SPIDER (35 fs pulses), where there is no ambiguity in the time direction, or with the GRENOUILLE (120 fs pulses). In the case of the GRENOUILLE device, we identified the temporal direction by performing a second measurement with additional known dispersion, as is usually done when using this apparatus. We observed that the GRENOUILLE spatial homogeneity requirements were fulfilled for the 120 fs laser by measuring the profile with a CCD. The spatial scan was performed with a motorized micrometric stage at the same time as the spectrum was acquired.

We first tested our system for one-dimensional SI, checking the reconstruction of laser pulses in comparison

with the SPIDER and GRENOUILLE characterizations. Among others, we performed a test in which the delay was varied from −5 to +5 ps in 50 fs steps, and we observed that the pulse intensity and phase were reconstructed independently of the delay over a wide range: up to several picoseconds. We also checked our reconstruction algorithm with simulations involving the characterization of complex pulses.

In general, interferometry is affected by small fluctuations due to system instabilities and, in particular, our fiber coupler approach was indeed expected to exhibit a phase drift. The consequence is a variation in the relative phase term between the two interferometer arms. Since this variation is almost independent of the wavelength, this means a loss of the constant zero-order relative phase of the pulses, thus preventing precise knowledge of the pulse wave-front and introducing a small error in the pulse front. For our purposes, this was not a problem and indeed there are techniques for overcoming this drawback and retrieving the wave-front from this kind of measurement [26]. We studied the stability of the interferences for single-shot measurements (acquired continuously without average), tracking the zero-order phase, the full spectral phase, the delay, and the time-width of the reconstruction. We measured a zero-order phase drift in the interferometer of 1.4 rad (peak to peak) during the time usually taken for a measurement to be made (about 1 min). The phase drift (0.45π) slightly affected the pulse front, with the corresponding temporal shift thus being limited to 0.60 fs ($0.225T$, with T being the laser period). For the delay, we calculated a standard deviation of 0.40 fs, and for the time-width of the measured pulse we calculated 0.09 fs, whereas the whole spectral phase was very stable between shots (except for the effect of the zero-order phase drift). We also studied stability for repeated multi-shot averaging measurements, for which we obtained blurry and reduced contrast interferences due to the shift of the fringes. As a result, more stable delays but poorer reconstructions were obtained due to incorrect phase retrieval.

B. Linear Chirp Experiments

In order to explore the limitations of our setup for the SI, we performed an experiment to measure the linear chirp. The test pulse was chirped through two passes in a diffraction-grating pair compressor using the 35 fs laser. We negatively chirped the pulse with group delay dispersion (GDD) varying from −7000 to −1000 fs^2 because these were the compressor limits for our setup. The linear chirp stretches the test pulse and this implies that the side-peaks in time of the Fourier-transform of the interferences broaden and decrease in amplitude. In our GDD scan, we varied the grating distance L and hence the GDD calculated as in [27] is

$$\mathrm{GDD}(L) \simeq -\frac{\lambda^3}{\pi c^2}\frac{L}{d^2\cos^2\theta_m}, \tag{2}$$

where λ is the central wavelength, c is the speed of light, $1/d = 300$ grooves/mm gives the groove density, and θ_m is the output angle calculated from the grating equation $\sin\theta_m - \sin\theta_0 = m\lambda/d$ (for the first order $m=1$ and the incidence angle in the grating $\theta_0 = 15°$). The GDD is linearly dependent on the grating distance and from Eq. (2) we calculated the estimated slope of $\mathrm{GDD}(L)/L = -212.8$ fs^2/mm. We measured the chirped pulses using the fiber coupler interferometer at 81 grating distances and reconstructed them with the FTSI. Thus, we obtained the spectral phase and calculated the experimental GDD from a quadratic fit as shown in Fig. 3(a), which corresponds to GDD = −5200 fs^2. In Fig. 3(b) the GDD is represented as a function of the grating distance. The linear regression of these data afforded a slope of −210.2 fs^2/mm, in very good agreement with the estimated value. Extrapolation of the fit to zero distance gives an acceptable deviation, $\mathrm{GDD}(L=0) = -28.7$ fs^2, and the correlation coefficient was $R = 0.999\,84$, revealing the good fit to the data. We also checked that the possible third-order dispersion (TOD) was completely negligible as compared to the GDD. Finally, we studied the instantaneous wavelength (as a function of the time) of the pulses, calculated from the electric field phase. In Fig. 3(c), using a false color scale, we plot the instantaneous wavelength of the pulses as a function of the grating distance. We have cropped the plot for the decrease in the pulse intensity greater than 3 orders of magnitude (shown in white). In this figure, we show the linear dependence on time of the instantaneous wavelength, explaining the pulse stretching. In Fig. 3(d), We represent the temporal reconstruction and instantaneous wavelength of the pulse corresponding to GDD = −5200 fs^2. We measured chirped pulses as long as 1.3 ps ($1/e^2$ width, decrease in the intensity to 13.5%) for the highest GDD. We also explored the intensity profile caused by the GDD (available at Media 1) and found that for the lowest chirps pulse splitting occurred due to the spectrum profile, but not to the TOD (negligible), which we also observed with the SPIDER measurements of the test pulse.

To further complete the results, we performed simulations using the experimental spectrum (bandwidth of 70 nm) and chirping the pulse with negative and positive GDDs up to 40,000 fs^2, always imposing our spectrometer resolution, and found that we could measure 7 ps long pulses ($1/e^2$ width). We also carried out simulations with the 120 fs laser spectrum with a GDD from −80,000 to 80,000 fs^2 and retrieved the input GDD and reconstructed 4 ps pulses ($1/e^2$ width).

One of the main advantages of the technique is its simplicity and robustness. These characteristics allow the reconstruction system to be adapted immediately to spectrometers or monochromators with much more resolution simply by plugging the fiber coupler to the input port of the device (common in most systems). Even though the whole spectral resolution of the spectrometer is not used, it is very easy to upgrade the STARFISH with commercial devices, with resolutions of around 0.02 nm for portable and small spectrometers in the visible and the infrared [capable of measuring Fourier-transform-limited narrowband pulses of 5 ps full width at half-maximum (FWHM), and even longer in the case of broadband chirped pulses], around 0.004 nm for optical spectrum analyzers and monochromators in the visible and the infrared (compatible with pulses of 25 ps FWHM), and even below 100 fm in the mid-infrared range, such as in the BOSA High-

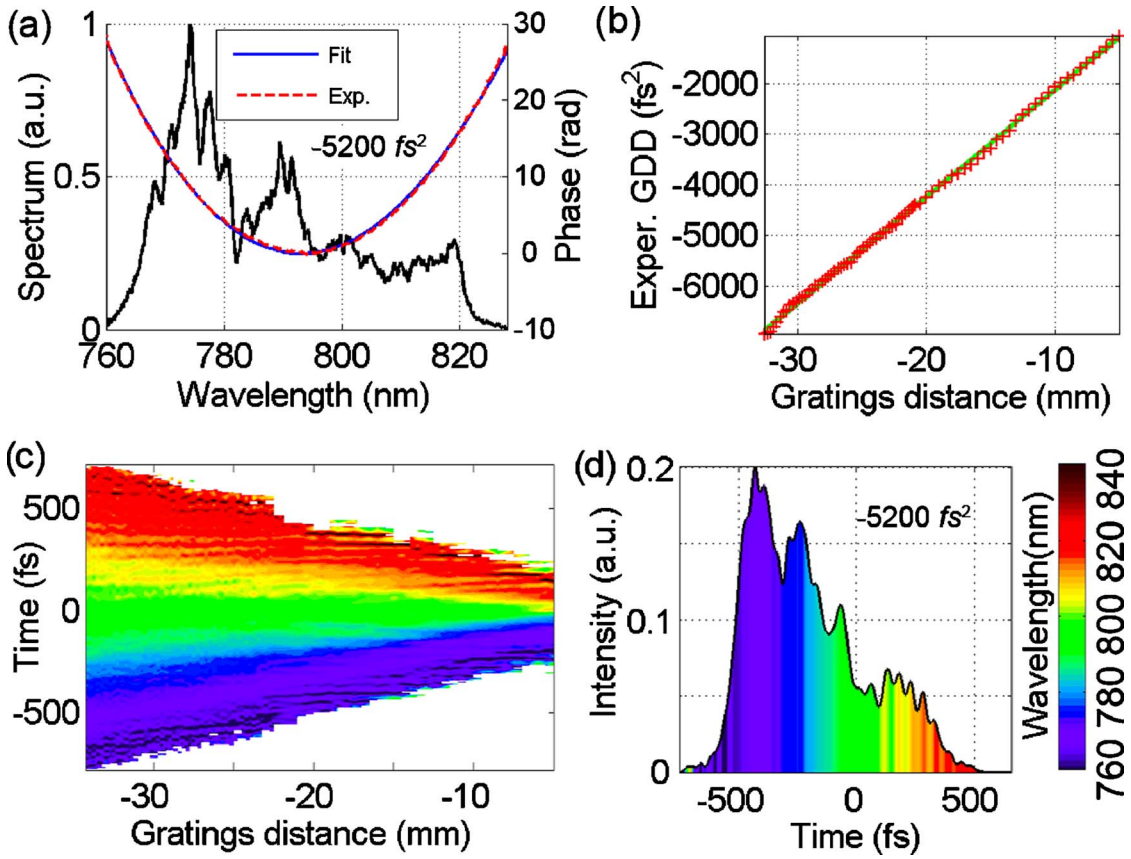

Fig. 3. (Color online) (a) Experimental spectrum and phase of a negatively chirped pulse. Experimental scan on negative linear chirp: (b) GDD retrieved from FTSI and (c) instantaneous wavelength of the chirped pulses as a function of the grating distance. (d) Temporal intensity and instantaneous wavelength of the chirped pulse. The intensity profile and instantaneous wavelength variation with the GDD can be seen in a video available at Media 1.

Resolution Optical Spectrum Analyzer (allowing unchirped pulses of 1 ns FWHM to be reconstructed).

C. Convergent Wave

The first spatiotemporal result reported here corresponds to a convergent wave using the 35 fs pulse duration laser focused by a 50 cm focal length lens (Fig. 4). The test beam (unknown beam) is scanned transversely 31 cm after the lens, that is, before the focus. In experiments with 35 fs pulses, the reference was calibrated with the SPIDER device. The delay between the reference and test beams was 550 fs. In Fig. 4(a), we show the spectral interference trace of the reference and test beams as a function of the wavelength and the transverse position. We scanned 4 mm of the beam profile in 20 μm steps (201 points). The evolution of the fringes with the position is quadratic, in agreement with the curvature of the wavefront and the pulse front of the test beam. The spatiotemporal intensity reconstruction is shown in Fig. 4(b), in which the convergence of the beam may be observed: the peripheral region of the beam arrives before the central region at a certain propagation distance. We fitted the retrieved pulse-front curvature of the beam [see fit in blue dashed line in Fig. 4(b)] and obtained a value of 18.6 cm for the radius of curvature, in agreement with the expected value of 19 cm, if Gaussian beam propagation is assumed.

Since we used a terawatt laser, the beam profile was inhomogeneous and the pulse energy fluctuated. To remove the energy instability, we have averaged the test beam spectrum taken at each point in the measurements presented in this work. We checked that the spectral phase retrieved was not affected by this instability. The intensity reconstruction showed in Fig. 4(b) exhibits spatial modulations that can be explained in terms of the spatial inhomogeneity of the beam. We checked that it was only due to the spatial profile by directly comparing the reconstruction with the Fourier-transform limit of the spatially

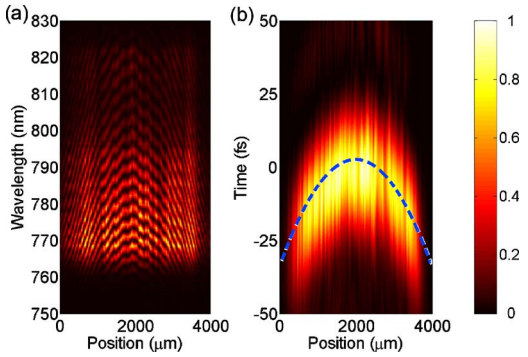

Fig. 4. (Color online) (a) Spatio-spectral interference trace and (b) spatiotemporal intensity reconstruction of a convergent wave (experimental, 35 fs pulses). The amplitude of the plots is in linear scale (see color scale on right).

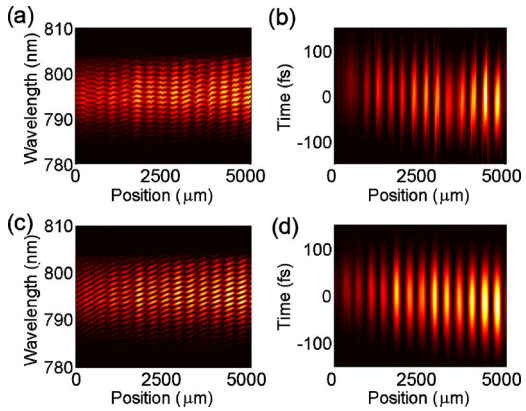

Fig. 5. (Color online) Experimental and simulated spatio-spectral interference traces [(a) experimental; (c) simulation] and spatiotemporal intensity reconstruction [(b) experimental; (d) simulation] of the interference between two crossing waves for 120 fs pulses.

resolved spectrum (where the FTSI cannot cause them). For further proof, we checked the reproducibility of the beam profile reconstruction, thus discarding the SI or laser instability as being the origin of the inhomogeneity of the reconstructed profile.

D. Spatiotemporal Interference of Two Plane Waves

The spatiotemporal interference of two ultrashort waves constitutes a more complex situation. To create the test beam, we formed a double-beam structure using a Mach–Zehnder interferometer before the test beam input arm of the fiber coupler. Both beams were first aligned and temporally overlapped. Then, we slightly crossed one beam with respect to the other, thus obtaining the spatial interferences of two crossing plane waves. In Fig. 5, we show the experimental results and simulations for this case using a different laser system of 120 fs pulses, also enabling us to reconstruct pulses with a narrower spectrum (FWHM of ~9 nm). In this case, we used the GRENOUILLE technique to characterize the reference that preserves the spatial homogeneity (required by the GRENOUILLE), because we split the laser beam before the Mach–Zehnder device. Figure 5(a) shows the interference spectrum trace, which displays two different fringe patterns: first, the fringes in the spectral dimension corresponding to the spectral interferences between the test beam and a 2.0 ps delayed reference beam, and second the fringes in the spatial dimension (13 maxima and minima) arising from the spatial interference of the two crossing waves that form part of the test beam. In this case, we scanned 5 mm of the beam profile in 20 μm steps (251 points). In the spatiotemporal intensity reconstruction [Fig. 5(b)] the two waves of the test beam had a delay of around zero and had slightly crossing pulse fronts (relative tilt of 36 fs for the 5 mm profile). The maxima and minima of the double wave reconstruction are due to the spatial interference of the beams. We performed the simu-

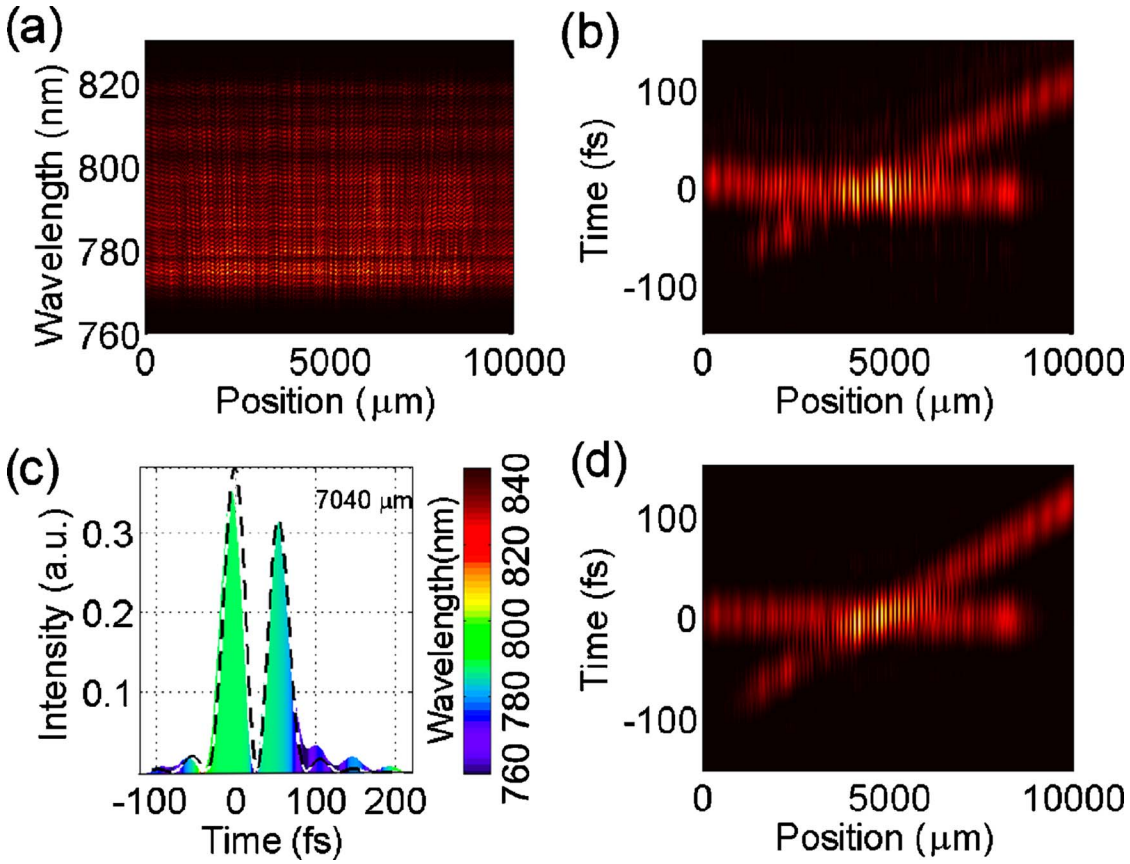

Fig. 6. (Color online) (a) Experimental spatio-spectral interference trace and spatiotemporal intensity reconstruction [(b) experimental; (d) simulation] of the interference of two crossing waves for 35 fs pulses. (c) Experimental temporal profile and instantaneous wavelength for the 7040 μm position in comparison with the simulated data (dashed line).

lations using parameters (spectrum, angle, and delay) extracted from the experimental conditions. The interference trace is shown in Fig. 5(c), and the intensity reconstruction is shown in Fig. 5(d). The simulations and the experiments are in good agreement, showing the same behavior.

We also implemented the previous experiment with the 35 fs pulse duration laser, obtaining interferences in a spectral bandwidth of 70 nm. We created the double beam with the Mach–Zehnder interferometer and controlled the relative angle and delay between the beams. In this case the delay between the test and reference beams was 2.0 ps. We then scanned 10,000 μm on a transverse axis of the beam in 20 μm steps (501 points). The experimental results and the corresponding simulations are shown in Fig. 6. The spatially resolved interference spectrum in Fig. 6(a) clearly shows the spectral interferences with the reference beam and the spatial interferences of the double wave forming the test pulse. The reconstruction of the spatiotemporal intensity [Fig. 6(b)] reveals two relatively crossed plane waves. The intensity has the characteristic structure of maxima and minima due to the spatial interferences of the two beams. In this experiment, the angle between the beams was sufficiently high to have 100 fs separated double pulses on both sides of the beam. In Fig. 6(c), we show the temporal profile of the double pulse corresponding to the position of 7040 μm colored with the instantaneous wavelength and compare with the simulated profile (dashed line), checking that there is no important chirp. Finally, we show the simulated intensity [Fig. 6(d)] with the parameters involved in the experiment. The simulations match the experimental reconstruction very well.

E. Spatiotemporal Interference of a Plane and a Spherical Wave

Finally, we measured the spatiotemporal interference of a spherical and a plane wave structure (Fig. 7). In this experiment, we used 35 fs laser pulses. We used a 50 cm focal lens in one arm of the Mach–Zehnder interferometer to obtain the spherical beam, whereas the other arm controlled the delay between the spherical and plane waves. The delay between the test and reference beams was 600 fs, whereas the spherical and plane waves overlapped in the central region. The spatio-spectral interference pattern of the spherical and plane waves can be seen in Fig. 7(a) (test beam trace, without the reference). We show the experimental interference spectral trace of the test and reference beams in Fig. 7(b), where the quadratic variation of the spectral fringes position due to the curvature of the spherical beam contribution (convergent) can be seen. This trace is the same as the test beam spectrum, with the only difference lying in the spectral fringes with the delayed reference pulse. The transverse scan of 4 mm was performed with 8 μm steps (501 points). The spatiotemporal intensity reconstruction [Fig. 7(c)] shows the interference of the spherical and plane waves: a modulated convergent beam is retrieved with maxima and minima in the profile. The spacing of this modulation is larger in the central than in the peripheral region, as corresponds to spherical and plane wave interference, and the same pattern was obtained in the simulation [Fig. 7(d)]. The relative delay between the spherical and plane beams was zero. We repeated this measurement for different relative delays between the plane and spherical waves up to 100 fs (above and below), such that in the reconstruction we see how both beams separate in time and the spatial interferences decrease. We also tested this situation with higher delays between the test and reference beams (1.0, 1.5, and 2.0 ps) and obtained the same intensity reconstructions.

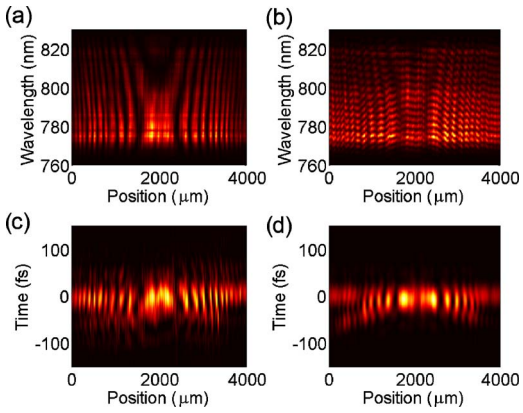

Fig. 7. (Color online) Spherical and plane wave interference for 35 fs pulses. Experimental (a) spatio-spectral test beam and (b) interference traces. (c) Experimental and (d) simulated spatiotemporal intensity reconstructions.

As discussed above, here we demonstrate the stability and reliability of the fiber coupler interferometer. The fluctuations in the experimental measurements and reconstructions in comparison with the simulations are not due to STARFISH limitations but to the laser beam shot-to-shot variations and the beam profile inhomogeneity, which are a consequence of using a terawatt laser with an amplification stage. The acquisition of a full spectral trace usually takes about 1 min, such that these variations of the laser pulses may introduce some noise into the reconstructions. Moreover, the use of a Mach–Zehnder interferometer for the double-beam structure has inherent instability and may cause fluctuations in the spatiotemporal interference experiments.

4. CONCLUSIONS

We propose a novel scheme for the spatiotemporal characterization of ultrashort laser pulses based on a fiber-optic coupler interferometer (STARFISH). The device has the advantages of being alignment-free, the fact that only one reference is used, and simplicity; only a fiber coupler and a standard spectrometer are necessary. The time direction is determined with this technique whenever it is known for the reference characterization, as in our case.

We have shown it to measure 1.3 ps long ($1/e^2$ width) negatively chirped pulses. According to the simulations, it could measure 1 ps FWHM unchirped pulses or, in the case of broadband chirped pulses, even longer ones. Moreover, the use of better resolution spectrometers allows the measurement of much longer pulses, conserving the advantages of the fiber coupler since it is only necessary to connect the fiber output to the spectrometer entrance. We applied the STARFISH not only to the characterization of a converging beam but also to more complex structures,

such as measurement of the spatiotemporal interference of plane-plane and spherical-plane waves, with the results obtained being in agreement with the simulations. We reconstructed laser beams using two laser systems with different pulse durations (35 and 120 fs) and spectral bandwidths. Despite working with terawatt lasers at 10 Hz, which do not have a perfectly homogeneous profile and are unstable, we demonstrate the ability of our method to reconstruct complex pulses. We expect this system to be used to characterize laser beams after they have undergone certain nonlinear processes or have passed through certain optical systems.

ACKNOWLEDGMENTS

The authors are grateful to S. Jarabo from the University of Zaragoza (Spain) for his assistance regarding the fiber coupler. We acknowledge support from Spanish Ministerio de Ciencia e Innovación (MICINN) through the Consolider Program SAUUL (CSD2007-00013), Research project FIS2009-09522 and from the Junta de Castilla y León through the Program for Groups of Excellence (GR27). We also acknowledge support from the Centro de Laseres Pulsados, CLPU, Salamanca, Spain. B. Alonso and I. J. Sola acknowledge support from the MICINN through the Formación de Profesorado Universitario and "Ramón y Cajal" programs, respectively.

REFERENCES

1. H. P. Weber, "Method for pulsewidth measurement of ultrashort light pulses generated by phase locked lasers using nonlinear optics," J. Appl. Phys. **38**, 2231–2234 (1967).
2. D. J. Kane and R. Trebino, "Characterization of arbitrary femtosecond pulses using frequency-resolved optical gating," IEEE J. Quantum Electron. **29**, 571–579 (1993).
3. C. Iaconis and I. A. Walmsley, "Spectral phase interferometry for direct electric-field reconstruction of ultrashort optical pulses," Opt. Lett. **23**, 792–794 (1998).
4. C. Froehly, A. Lacourt, and J. Ch. Vienot, "Notion de réponse impulsionnelle et de fonction de transfert temporelles des pupilles optiques, justifications expérimentales et applications," Nouv. Rev. Opt. **4**, 183–196 (1973).
5. J. Piasecki, B. Colombeau, M. Vampouille, C. Froehly, and J. A. Arnaud, "Nouvelle méthode de mesure de la réponse impulsionnelle des fibres optiques," Appl. Opt. **19**, 3749–3755 (1980).
6. D. N. Fittinghoff, J. L. Bowie, J. N. Sweetser, R. T. Jennings, M. A. Krumbügel, K. W. DeLong, R. Trebino, and I. A. Walmsley, "Measurement of the intensity and phase of ultraweak, ultrashort laser pulses," Opt. Lett. **21**, 884–886 (1996).
7. R. V. Shack and B. C. Platt, "Production and use of a lenticular Hartmann screen," J. Opt. Soc. Am. **61**, 656–660 (1971).
8. L. Gallmann, G. Steinmeyer, D. H. Sutter, T. Rupp, C. Iaconis, I. A. Walmsley, and U. Keller, "Spatially resolved amplitude and phase characterization of femtosecond optical pulses," Opt. Lett. **26**, 96–98 (2001).
9. A. Zaïr, A. Guandalini, F. Schapper, M. Holler, J. Biegert, L. Gallmann, A. Couairon, M. Franco, A. Mysyrowicz, and U. Keller, "Spatio-temporal characterization of few-cycle pulses obtained by filamentation," Opt. Express **15**, 5394–5405 (2007).
10. S. Akturk, M. Kimmel, P. O'Shea, and R. Trebino, "Measuring pulse-front tilt in ultrashort pulses using GRENOUILLE," Opt. Express **11**, 491–501 (2003).
11. J. Jasapara, "Characterization of sub-10-fs pulse focusing with high-numerical-aperture microscope objectives," Opt. Lett. **24**, 777–779 (1999).
12. P. Bowlan, P. Gabolde, and R. Trebino, "Directly measuring the spatio-temporal electric field of focusing ultrashort pulses," Opt. Express **15**, 10219–10230 (2007).
13. J. Trull, O. Jedrkiewicz, P. Di Trapani, A. Matijosius, A. Varanavicius, G. Valiulis, R. Danielius, E. Kucinskas, A. Piskarskas, and S. Trillo, "Spatiotemporal three-dimensional mapping of nonlinear *X* waves," Phys. Rev. E **69**, 026607 (2004).
14. D. Faccio, A. Matijosius, A. Dubietis, R. Piskarskas, A. Varanavičius, E. Gaizauskas, A. Piskarskas, and A. Couairon, "Near- and far-field evolution of laser pulse filaments in Kerr media," Phys. Rev. E **72**, 037601 (2005).
15. D. E. Adams, T. A. Planchon, A. Hrin, J. A. Squier, and C. G. Durfee, "Characterization of coupled nonlinear spatiospectral phase following an ultrafast self-focusing interaction," Opt. Lett. **34**, 1294–1296 (2009).
16. S. A. Diddams, H. K. Eaton, A. A. Zozulya, and T. S. Clement, "Full-field characterization of femtosecond pulses after nonlinear propagation," in *Conference on Lasers and Electro-Optics (CLEO/US)*, Vol. 6 of OSA Technical Digest Series (Optical Society of America, 1998), paper CFF3.
17. B. Alonso, I. J. Sola, O. Varela, C. Mendez, I. Arias, J. San Román, A. Zaïr, and L. Roso, "Spatio-temporal characterization of laser pulses by spatially resolved spectral interferometry," Opt. Pura Apl. **43**, 1–7 (2010).
18. S. Rivet, L. Canioni, R. Barille, and L. Sarger, "Multidimensional shearing for linear and nonlinear propagation analysis," in *Ultrafast Optics Conference* (2001), paper M20.
19. E. Rubino, D. Faccio, L. Tartara, P. K. Bates, O. Chalus, M. Clerici, F. Bonaretti, J. Biegert, and P. Di Trapani, "Spatiotemporal amplitude and phase retrieval of space-time coupled ultrashort pulses using the Shackled-FROG technique," Opt. Lett. **34**, 3854–3856 (2009).
20. C. Dorrer, E. M. Kosik, and I. A. Walmsley, "Direct space–time characterization of the electric fields of ultrashort optical pulses," Opt. Lett. **27**, 548–550 (2002).
21. P. Gabolde and R. Trebino, "Single-shot measurement of the full spatio-temporal field of ultrashort pulses with multispectral digital holography," Opt. Express **14**, 11460–11467 (2006).
22. P. Bowlan, P. Gabolde, A. Shreenath, K. McGresham, R. Trebino, and S. Akturk, "Crossed-beam spectral interferometry: a simple, high-spectral-resolution method for completely characterizing complex ultrashort pulses in real time," Opt. Express **14**, 11892–11900 (2006).
23. D. Meshulach, D. Yelin, and Y. Silberberg, "Real-time spatial–spectral interference measurements of ultrashort optical pulses," J. Opt. Soc. Am. B **14**, 2095–2098 (1997).
24. A. S. Wyatt, I. A. Walmsley, G. Stibenz, and G. Steinmeyer, "Sub-10 fs pulse characterization using spatially encoded arrangement for spectral phase interferometry for direct electric field reconstruction," Opt. Lett. **31**, 1914–1916 (2006).
25. L. Lepetit, G. Cheriaux, and M. Joffre, "Linear techniques of phase measurement by femtosecond spectral interferometry for applications in spectroscopy," J. Opt. Soc. Am. B **12**, 2467–2474 (1995).
26. P. R. Bowlan, M. Lõhmus, P. Piksarv, H. Valtna-Lukner, P. Saari, and R. Trebino, "Measuring the spatio-temporal field of diffracting ultrashort pulses," in *Frontiers in Optics*, OSA Technical Digest (CD) (Optical Society of America, 2009), paper FTuO5.
27. E. B. Treacy, "Optical pulse compression with diffraction gratings," IEEE J. Quantum Electron. **5**, 454–458 (1969).